Solution process of graphene-induced ohmic contact between the metal and AlGaN/GaN for hemts application

Tran Viet Cuong[1], Anh Hao Huynh Vo[2, 3], The Duy Nguyen[1], Duc Anh Dinh[1], Trung Tin Tran[3, 4, 5, *], Trung Nghia Tran[2, 3, *]

[1]*VKTECH Research Center, NTT Hi-Tech Institute, Nguyen Tat Thanh University, 298-300A Nguyen Tat Thanh Street, Ward 13, District 4, Ho Chi Minh City, Viet Nam*

[2]*Laboratory of Laser Technology, Faculty of Applied Science, Ho Chi Minh City University of Technology (HCMUT), 268 Ly Thuong Kiet Street, District 10, Ho Chi Minh City, Viet Nam*

[3]*Vietnam National University Ho Chi Minh City, Linh Trung Ward, Thu Duc, Ho Chi Minh City, Viet Nam*

[4]*Department, of Engineering Physics, Faculty of Applied Science, Ho Chi Minh City University of Technology, 268 Ly Thuong Kiet Str., Dis. 10, Ho Chi Minh City, Viet Nam*

[5]*Faculty of Physics and Physics Engineering, University of Science, 268 Ly Thuong Kiet Str., Dis. 10, Ho Chi Minh City, Viet* Nam

[*]Emails: *1.ttnghia@hcmut.edu.vn, 2.trtrtin@hcmut.edu.vn*

Received: 25 December 2023; Accepted for publication: 29 March 2024

Abstract. This work demonstrates an AlGaN/GaN high electron mobility transistor (HEMT) with Cr/Graphene ohmic contacts constructed without heat treatment. The Cr/Graphene ohmic contact was fabricated using a spray-coated graphene nanoflakes solution and electron-beam-evaporated Cr. This method does not require a high-temperature annealing step in conventional Ti/Al/Ni/Au ohmic contact. It is suggested that the Cr/graphene combination acts similarly to a doped n-type semiconductor in contact with AlGaN/GaN heterostructures, enabling carrier transport to the AlGaN layer. The investigated Au/Cr/ Graphene/AlGaN/GaN HEMT device exhibits ohmic drain characteristics in the range of -4 V to 4 V of drain-source voltage with a calculated contact resistance density of 2.5 $m\Omega cm^2$. Our results have important implications for the fabrication and manufacturing of AlGaN/GaN-based microelectronic and optoelectronic devices/sensors of the future.

Keywords: high electron mobility transistors (HEMTs), graphene, AlGaN/GaN, ohmic contact.

Classification numbers: 2.4.1, 2.5.2.

1. INTRODUCTION

HEMTs, short for High Electronic Mobility Transistors, are a progressive platform of field-effect transistors that can operate at high frequency in extreme voltage and temperature

conditions [1-5]. These types of transistors consist of a crucial planar heterojunction called a two-dimensional electron gas (2DEG) formed by combining two semiconductors. The electrons are portrayed as majority charge carriers capable of free movement in the 2DEG planar region. Because of this exceptional system, the HEMT exhibits characteristics better than conventional transistors in high switching speed, high gain, and low noise signal. Although the initial ambition in the development related to high-speed communication applications, due to their superior physical properties, HEMTs also open potential applications in power electronics, vehicles, or space [6].

The HEMTs based on Gallium Nitride (GaN) are considered a promising candidate for high-power and high-frequency applications due to the excellent properties of wide band gap semiconductor materials in recent years [7]. Due to the high breakdown electric field and electron velocity, AlGaN/GaN heterostructure field-effect transistors reveal greater advantages in high-power radio frequency (RF) applications. The maximum oscillation frequency and breakdown voltage of the AlGaN/GaN HEMT devices have been reported to be 380 GHz and 2900 V, respectively [8].

Besides the outstanding advantages mentioned, these platforms still have limitations. Ohmic contacts to AlGaN/GaN heterostructures usually require multilayer metallization (typically Ti/Al/Ni/Au) and annealing at high temperatures because of the large Schottky barrier height at the metal/AlGaN/GaN interface. To induce these Ohmic contacts, the conventional annealing temperature is used above 850 ^{o}C to optimize the contact resistance [9]. Such Ohmic contacts are known to reduce device reliability, limit the minimum device size, and add to the complexity of the processing. Park *et al.* demonstrated an option for fabricating Ohmic contact without a high-temperature annealing process. By inserting a single layer chemical vapor deposition (CVD) graphene between the Cr and AlGaN/GaN layers, a low resistive contact with the AlGaN/GaN heterostructures is formed [10]. However, the graphene transfer process is also relatively complicated due to the need for high-temperature CVD graphene growth (usually at 1000 °C).

In this work, we proposed another choice to form ohmic contact by creating Cr/Graphene layers for AlGaN/GaN HEMT based on the graphene liquid process using sonication. In this way, the efficiency of HEMT manufacturing is improved because of the omission of the steps involved in high temperatures.

2. MATERIALS AND METHODS

2.1. Solution-based graphene synthesis

Graphene nanoflakes dispersed in N-methylpyrrolidone (NMP) were synthesized via liquid phase exfoliation of graphite precursor. Detailed implementation steps are shown in Figure 1. First, 500 mg graphite was dispersed in 50 ml of NMP solvent. The mixture was then subjected to an ultrasonic cleaner for 6 hours at a power of 300 W to extract individual graphene layers using the frequency of 45 kHz. During the sonication process, a circulating water thermostat was used and set at 25 °C to avoid a temperature increase caused by energy accumulation. The graphite was exfoliated and dispersed in NMP solvent because of the pressure elevated by ultrasonic waves inside the solution. It should be noted that NMP with a surface tension of about 40 mN/m. At this tension value, the graphite's exfoliation process is the best due to the minimized interfacial tension between the solvent and the graphene layer [11]. As a result, the exfoliation efficiency is about 80 %. The as-synthesized mixture was then centrifuged at 5000

rpm for 20 minutes. The graphene supernatant was collected and unexfoliated graphite precipitation was discarded. The synthesized graphene was finally transferred to a nontoxic solvent, a mixture of ethanol and deionized water with a ratio of 80:20 to produce the graphene dispersion.

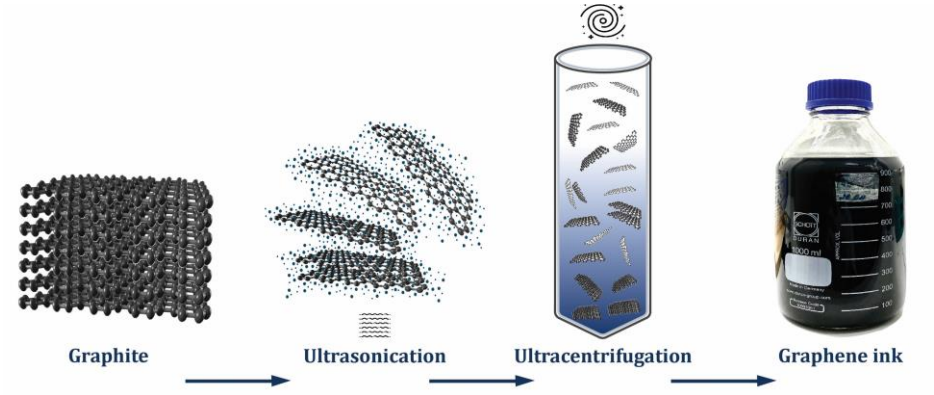

Figure 1. Graphene synthesis process based on solution method.

The synthesized graphene solution was spun or spray-coated on a quartz substrate for characterization. Herein, graphene sheet morphology and size were investigated using transmission electron microscopy (TEM) and atomic force microscopy (AFM). The crystal quality was studied using the SPEX 1403 Raman spectrometer with an excitation wavelength of 632.8 nm using a He-Ne laser at 1 mW of power.

2.2. Device Fabrication and Measurement

In this study, the $Al_{0.25}Ga_{0.75}N$/GaN heterostructures were epitaxially grown on sapphire substrates using a metal-organic chemical vapor deposition (MOCVD) system. Trimethylaluminum (TMAl) and trimethylgallium (TMGa) are the metal organic sources of Al and Ga. H_2 acts as the carrier gas, and ammonia serves as the N precursor. Initially, the chamber underwent a high-temperature (1100 °C) with H_2 flow wash, followed by a cooling process to 550 °C to facilitate the formation of a 30-nm-thick GaN buffer layer. To create the AlGaN/GaN heterostructure, a 1μm-thick GaN and 25-nm-thick AlGaN were produced at 1100 °C. TMAl and TMGa flow rates were 50 μmol/min and 20 μmol/min, respectively, while the GaN and AlGaN layers were produced at a pressure of 50 Torr. The III/V ratio was changed in order to optimize the Al composition to be 0.25. The schematic of the HEMT device is shown in Figure 2. The HEMT fabrication started with the mesa isolation process using inductively coupled plasma etching. The source and drain areas were created using conventional photolithography. Before photolithography, 2 ml of graphene solution with a concentration of 0.025 mg/mL was spray coated on top. Thereafter, a Cr/Au (30:100 nm) metal electrode was deposited by electron beam evaporation. A sample with only Cr/Au contact but no graphene was also produced for comparison. The fabricated HEMT structure has a dimension of 100 μm × 70 μm, with a gate source and gate-drain spacing of 5 μm and a gate length of 10 μm, respectively. Current-voltage (I-V) measurements were performed using a semiconductor parameter analyzer (Keithley 4200) and a source meter (Keithley 2420).

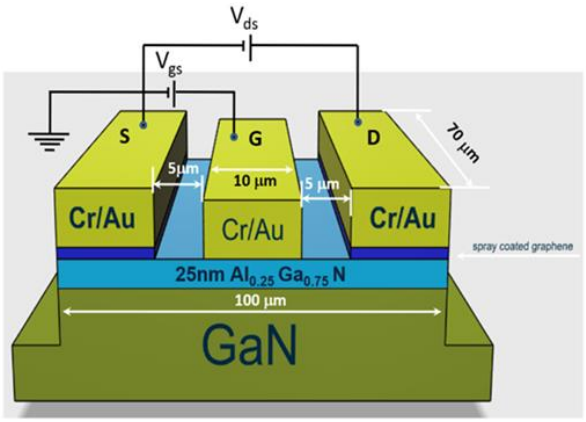

Figure 2. Schematic diagram of the fabricated Cr/Au/Graphene/AlGaN/GaN HEMT

3. RESULTS AND DISCUSSION

3.1. Graphene Characterization

The Raman spectrum of graphene synthesized by the liquid sonication process is shown in Figure. 3, with an inset picture of the graphene solution. The main peaks obtained with the characteristics of graphene include the G peak (~ 1580 cm^{-1}) and the 2D peak (~ 2700 cm^{-1}), corresponding to Raman scattering of the first and second order, respectively. This spectrum graph also shows two small peaks, the 2D' peak (~ 3200 cm^{-1}) and the D + D" peak (~ 2450 cm^{-1}), which are related to the two-phonon vibration process of graphene. Furthermore, the presence of peaks D, D’ and D + D" at wavenumbers around 1350 cm^{-1}, 1650 cm^{-1}, and 2950 cm^{-1} in the spectrum indicates that the synthesized graphene still has defects. These commented peaks are related to graphene with defects that were reported in the previous report [12].

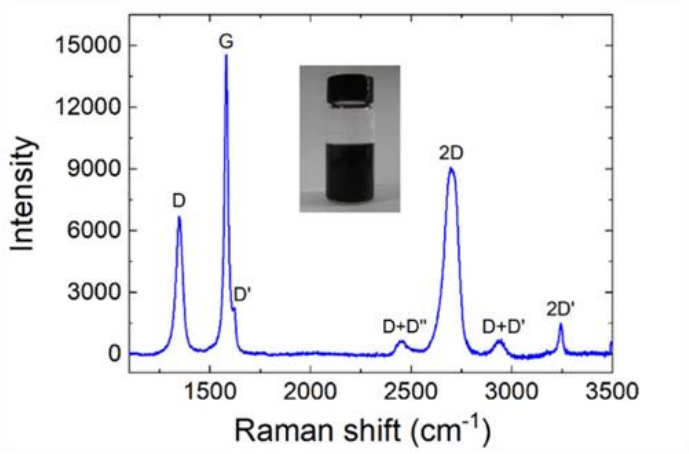

Figure 3. Raman spectrum of solution-based synthesis of Graphene.

In addition to the peak positions, the ratio of the 2D peak intensity (I_{2D}) and the G peak intensity (I_G) is a crucial factor in the investigation of graphene. The ratio of I_{2D}/I_G in the Raman spectroscopy of the synthesized graphene exceeds one, suggesting that the graphene sample has

multilayers [13]. Specifically, the sample morphology is nanoflakes, which is clearly illustrated in Figure 4. This result is due to the cavitation phenomenon that occurs in the sonication process. During the ultrasonic graphene treatment, the compression and rarefaction cycles caused by ultrasound lead to the generation of vacuum bubbles in the solution. When the bubbles cannot gain more energy, they implode in the next compression cycle. Cavitation bubbles can reach a temperature of 5000 K and a pressure of 1000 bars within them [14]. This particular series of events provides the trigger for graphite exfoliation to graphene nanoflakes.

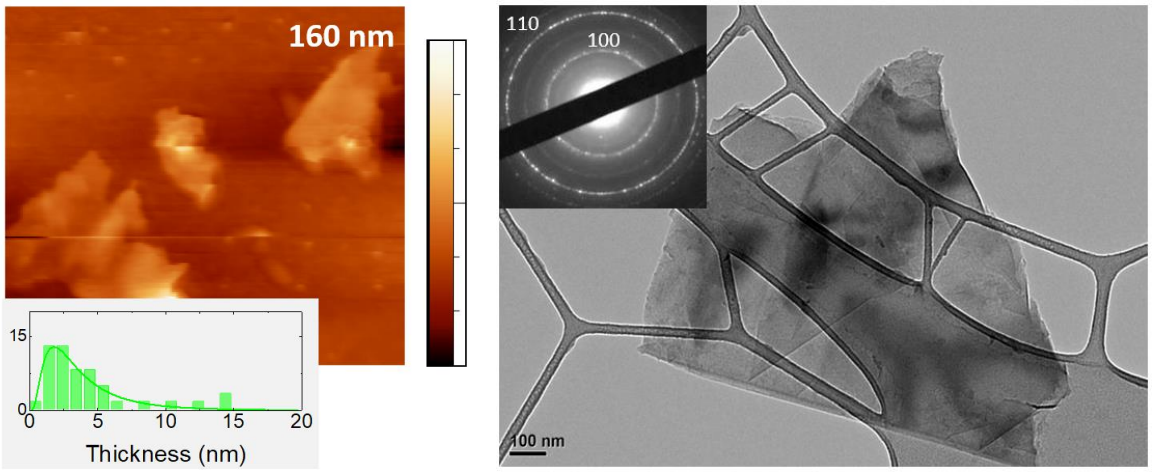

(a) (b)

Figure 4. (a) AFM topography with the inset of graphene thickness distribution and (b) TEM image with inset SAED pattern of synthesized graphene nanoflake.

Figure 4(a) presents the AFM topography of the synthesized graphene, with the inset showing the distribution of graphene thickness. The majority of synthesized graphene nanoflakes are sub-6 nm in size, with the most frequent sizes being 2 and 3 nanometers, corresponding to 4 - 5 graphene layers as confirmed by the SEM image in Figure 4(b). Furthermore, the similar surface energy of NMP to graphene [15] and the sonication temperature of 25 °C contribute to the stability of the peeling process by limiting graphene aggregation.

3.2. HEMT Characterizations

$Al_{0.25}Ga_{0.75}N$/GaN HEMT using Cr/Graphene as ohmic contacts are denoted as GHEMT. The drain characteristics at 1 V gate source voltage (V_{gs}) of GHEMT and the reference sample (without graphene) measured by the Keithley 2420 source meter are shown in Figure 5. As a result, Schottky behavior was demonstrated in the reference sample, as evidenced by the pinch-off region in the drain-source voltage (V_{ds}) range from -4 V to 4 V. Conversely, in this V_{ds} region, the behavior of GHEMT's drain characteristic is ohmic-like. Using the transfer length measurement (TLM), the contact resistance density is calculated to be approximately 2.5 $m\Omega cm^2$. As previously reported [16], the Schottky barrier height for Graphene/AlGaN contacts ranges from 1.25 eV to 1.53 eV for Al mole fractions of 0.15 to 0.4. Therefore, we suggest that the ohmic behavior of GHEMT is due to the formation of a doped n-type semiconductor layer with a non-zero band gap at the Graphene/Cr interface, which allows carriers to transport to the AlGaN layer.

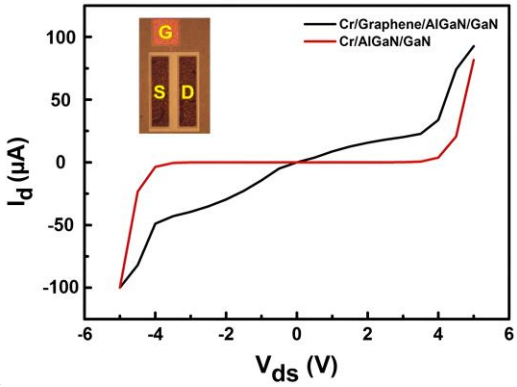

Figure 5. Current - Voltage (Id-Vds) characteristics of GHEMT and the sample without graphene with the inset showing the top view of the fabricated devices.

The output and transfer characteristics of GHEMT are shown in Figure 6. In particular, Figure 6(a) indicates the drain current-drain voltage characteristics of the GHEMT device with varying gate bias, confirming that the device is operating as expected. The V_{ds} are swept from 0 V to 10 V with a step of 0.5 V. When V_{gs} = 1 V, the maximum drain current is slightly more than 0.8 mA with the V_{ds} = 6 V. This low drain current is due to the higher contact resistance of the GHEMT device compared to conventional HEMT (around 10 $\mu\Omega cm^2$). Additionally, GHEMT also shows stability without the appearance of kinks and negative slope effects. On the other hand, the transconductance (g_m) (dI_{ds}/dV_{gs}) and I_{ds} versus the gate voltage of GHEMT are shown in Figure 6(b) with the swept voltage in the range from -8 V to 1 V at V_{ds} = 3 V. The transconductance curve indicates that the maximum g_m value is approximately 0.725 mS, corresponding to the gate source voltage at 0 V. The linear behavior caught from the transfer curve is in the region from -4 V to -2 V with the pinch-off point at V_{gs} = -4 V.

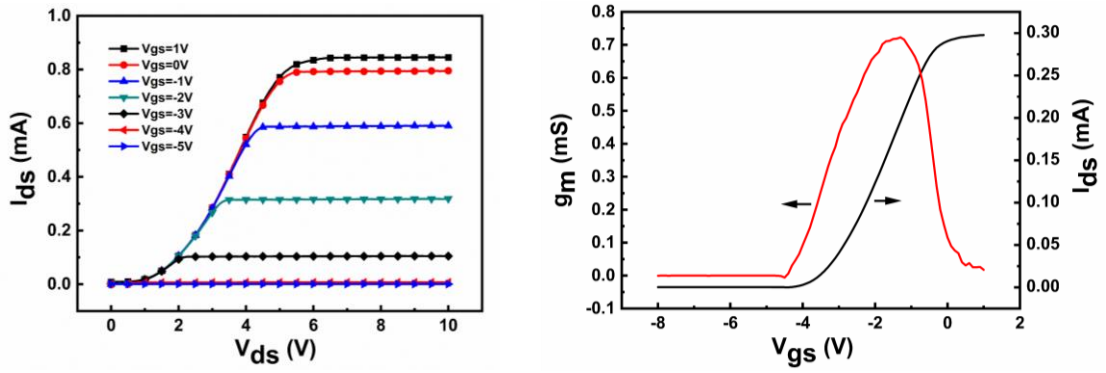

(a) (b)

Figure 6. (a) DC I_{ds} – V_{ds} characteristics and (b) Transfer curves of fabricated GHEMT

4. CONCLUSIONS

For the HEMT device, we have fabricated and characterized the Metal/Graphene/AlGaN/GaN ohmic contact. Here, graphene is produced via a solution-based approach, which is less expensive and complex than traditional procedures, which typically call for additional high-temperature heating treatment. Our results show that the synthesized

graphene was found to be in a nanoflake form with about 4 to 5 layers. The GHEMT device fabricated with these nanoflakes exhibited ohmic behavior in the V_{ds} region from -4 V to 4 V, while the reference sample without graphene showed Schottky behavior in the same region. The contact resistance of GHEMTs (2.5 $m\Omega cm^2$) is higher than that of conventional HEMTs (10 $\mu\Omega cm^2$). However, this can be improved by optimizing the graphene solution and spraying parameters. Our method has great potential in the fabrication of AlGaN electronic devices because it is a less expensive and less complicated alternative to conventional methods.

Acknowledgements. This research is funded by Vietnam National University Ho Chi Minh City (VNU-HCM) under grant number B2022-20-01/HĐ-KHCN. We acknowledge Ho Chi Minh City University of Technology (HCMUT), and VNU-HCM for supporting this study.

Credit authorship contribution statement. Tran Viet Cuong: Methodology and investigation. Anh Hao Huynh Vo: Formal analysis and writing-original draft and. The Duy Nguyen: Formal analysis. Duc Anh Dinh: Methodology and investigation. Trung Tin Tran: supervision. Trung Nghia Tran: Funding acquisition and supervision.

Declaration of competing interest. The authors declare that they have no known competing financial interests or personal relationships that could have appeared to influence the work reported in this paper.

REFERENCES

1. Ma C. T., Gu Z. H. - Review of GaN HEMT Applications in Power Converters over 500 W, Electronics **8** (2019) 1401.
2. Yu C., Wang F., He J., Zhang Y., Sun R., Xu W., Ding G., Feng Q., Wang X., Wang Y., He M., Chen W., Jia H., Chen H. - High Voltage Normally-Off p-GaN Gate HEMT with the Compatible High Threshold and Drain Current, ECS Journal of Solid State Science and Technology **11** (2022) 085009.
3. Remesh N., Chandrasekar H., Venugopalrao A., Raghavan S., Rangarajan M., Nath D. N. - Re-engineering transition layers in AlGaN/GaN HEMT on Si for high voltage applications, Journal of Applied Physics **130** (2021)
4. Sahebghalam N., Shalchian M., Chalechale A., Jazaeri F. - High-Temperature HEMT Model, IEEE Transactions on Electron Devices **69** (2022) 4821-4827.
5. Lu S., Burgos R., Lu G. Q. - Packaging and high-temperature characterization of a 650 V, 150 A eGaN HEMT, Semiconductor Science and Technology **36** (2021) 034006.
6. Islam N., Mohamed M. F. P., Khan M. F. A. J., Falina S., Kawarada H., Syamsul M. - Reliability, Applications and Challenges of GaN HEMT Technology for Modern Power Devices: A Review, Crystals **12** (11) (2022)1581.
7. Haziq M., Falina S., Manaf A. A., Kawarada H., Syamsul M. - Challenges and Opportunities for High-Power and High-Frequency AlGaN/GaN High-Electron-Mobility Transistor (HEMT) Applications: A Review, Micromachines **13** (2022) 2133.
8. Mounika B., Ajayan J., Bhattacharya S., Nirmal D. - Recent developments in materials, architectures and processing of AlGaN/GaN HEMTs for future RF and power electronic applications: A critical review, Micro and Nanostructures **168** (2022) 207317.
9. Chen D., Wan L., Li J., Liu Z., Li G. - Ohmic contact to AlGaN/GaN HEMT with electrodes in contact with heterostructure interface, Solid-State Electronics **151** (2019) 60-64.

10. Sung Park P., Reddy K. M., Nath D. N., Yang Z., Padture N. P., Rajan S. - Ohmic contact formation between metal and AlGaN/GaN heterostructure via graphene insertion, Applied Physics Letters **102** (2013)
11. Chem T., Moosa A., Abed M. - Graphene preparation and graphite exfoliation, Turkish Journal of Chemistry **45** (2021) 493-519.
12. Reichardt S., Wirtz L. - Raman Spectroscopy of Graphene, arXiv: Mesoscale and Nanoscale Physics (2017)
13. InstaNANO, Graphene Number of Layers Calculator From ID/IG and I2D/IG Ratio via Raman Spectroscopy, https://instanano.com/all/characterization/raman/graphene-layers/ (accessed 1st September 2023).
14. Sarac B., Stephens D., Eisener J., Rosselló J., Mettin R. - Cavitation bubble dynamics and sono chemiluminescence activity inside sonicated submerged flow tubes, 2020.
15. Arao Y., Mori F., Kubouchi M. - Efficient solvent systems for improving production of few-layer graphene in liquid phase exfoliation, Carbon **118** (2017)
16. Pandit B., Seo T., Ryu B., Cho J. - Current transport mechanism in graphene/AlGaN/GaN heterostructures with various Al mole fractions, AIP Advances **6** (2016) 065007.